EXAFS Spectra of the Dilute Solutions of Ca^{2+} and Sr^{2+} in Water and Methanol

Liem X. Dang,* Gregory K. Schenter,* and John L. Fulton*

Chemical Sciences Division, Pacific Northwest National Laboratory, Richland, Washington 99352

Received: August 12, 2003; In Final Form: October 7, 2003

A set of polarizable ion−water intermolecular potential models were developed that accurately describe solvation enthalpies and structural properties of Ca^{2+} and Sr^{2+} in aqueous solution. The molecular dynamics (MD) results were coupled to electron scattering simulations in order to generate the Ca^{2+} and Sr^{2+} extended X-ray absorption fine structure (EXAFS) spectra. These MD-XAFS spectra were found to be in good agreement with the corresponding experimental measurements including both the ion-oxygen and the ion-hydrogen distances for the first hydration shell. This work demonstrates that the combination of MD-EXAFS, and the corresponding experiment measurement provides a powerful tool in the analysis of the solvation structure of aqueous ionic solutions. The Ca^{2+}−methanol interaction was also developed, and the dilute Ca^{2+} MD-EXAFS spectrum in liquid methanol was also predicted using the same approach.

I. Introduction

Computer simulation techniques, such as molecular dynamics (MD), are powerful tools in the analysis of the chemical and physical properties of solvated ions in solution.[1] An accurate description of molecular interactions remains an active research field, even though substantial efforts have been made in this area. Potential parameters employed in computer simulations are usually constructed using data obtained from experiments (i.e., hydration enthalpy and/or free energy of solvation) and/or data from accurate ab initio calculations. Subsequently, the results predicted by computer simulations can be validated and improved by comparison with the corresponding experimental measurements such as partial structural factors and EXAFS spectra.

In this paper, we present a detailed MD simulation of solvation structures of dilute Ca^{2+}- and Sr^{2+}−water solutions. The hydrated Ca^{2+} plays an important role in many biological processes, such as Ca^{2+} binding to proteins or membranes.[2] A detailed study of the solvation structure of the Sr^{2+}−water solution, due to its environmental importance, can significantly enhance our understanding of the mobility of toxic metal contaminants in groundwater.[3] Toward this end, we have developed a set of polarizable ion−water interactions (i.e., Ca^{2+}−water and Sr^{2+}−water) that accurately describes hydration enthalpies, coordination numbers, and the peak locations of the ion water radial distribution functions. Subsequently, the MD EXAFS spectra were calculated and compared to the corresponding experimental measurements including both the ion−oxygen and the ion−hydrogen distance for the first hydration shell. Using this same approach, we also computed the MD-EXAFS of the dilute Ca^{2+} EXAFS in liquid methanol.

We employed polarizable models, so that the ion−water interactions could be described more accurately and the water molecules would respond to the electric fields create by their environments, in a realistic way (i.e., increasing in the dipole moments).[4] In recent years, MD simulations have been used to simulate EXAFS spectra for ions in solution. These studies include the MD simulations of Palmer and co-workers[5] directly modeling the EXAFS spectra of strontium chloride solutions and the MD simulations of Hermansson and co-workers[6] directly modeling the EXAFS spectra of calcium chloride solutions. Another significant contribution to this subject is the work of Berendsen and co-workers[7] on simulations of the EXAFS spectrum of dilute Sr^{2+} in liquid methanol.

Pair potential models were used in the above-mentioned studies. A major conclusion of these studies was that, although the simulated spectra are in nearly quantitative agreement with experimental data, the observed deviations from the experimental data most likely come from a deficiency in the MD model (i.e., potential models). The paper is organized as follows. The polarizable model potentials and the simulation methods are summarized in section II. The results are presented and discussed in section III. Our conclusions and discussion of future research directions are given in section IV.

II. Potential Models and Simulation Methods

(a) Potential Model. We employed the rigid-body polarizable water model of Dang and Chang to describe the water−water intermolecular interaction.[8] The functional form of the empirical potential includes a sum of Lennard-Jones (r^{-6} and r^{-12}), Coulombic interactions and a polarization term in order to account for many body effects. This model describes reasonably well the structure and thermodynamic properties of the bulk and the liquid/vapor interface of water. The polarizable potential parameters for the ion−water interactions were developed to reproduce the experimental solvation enthalpy and the structural properties of solvated ions in liquid water. The results are discussed in following section.

(b) Simulation Methods. The MD simulations for this system consisted of 600 water molecules and an ion in a cubic simulation cell with a linear dimension roughly equal to 26.3 Å per side. Periodic boundary conditions were applied in all three dimensions. The simulations were carried out in an isobaric−isothermal (NPT) ensemble at 1 atm and 298 K, with time steps for heat bath coupling and pressure relaxation of 0.1 and 0.2 ps, respectively.[9] The SHAKE algorithm[10] is used during the entire simulation to constrain all the bond lengths in order to fix the water internal geometry. Ewald summation techniques

* To whom correspondence should be addressed.

10.1021/jp030968s CCC: $25.00
Published on Web 11/19/2003

TABLE 1: Potential Parameters for H_2O, Ca^{2+}, and Sr^{2+} Used in MD Simulations

molecule	atom type	σ(Å)	ϵ(kcal/mol)	q (e)	α(Å^3)
H_2O	H	0.000	0.0000	0.5190	0.000
	O	3.234	0.1825	0.0000	0.000
	M	0.000	0.0000	−1.0380	1.444
Ca^{2+}	Ca	2.9132	0.1000	2.0000	0.470
Sr^{2+}	Sr	3.1671	0.1000	2.0000	0.860

should be used to evaluate the long-range interactions in polar systems.[1] However, in the present work, we focused on the solvation properties associated with the short-range ion−water interactions (i.e., first and second solvation shells) of an infinitely dilute solution. Therefore, the nonbonded (i.e., short-range Lennard-Jones, long-range charge−charge, charge−dipole, and dipole−dipole) interactions were truncated at a molecular separation of 9 Å; the system size with an appropriate molecule−molecule based cutoff distance was chosen to ensure that the computed quantities presented in this paper would be comparable to the simulations that were based on Ewald summation techniques.[11] In all MD simulations, a time step of 2 fs was used. After an energy minimization to relax the initial coordinates, the simulation was carried out to 300 ps to equilibrate the system, followed by at least 300 ps of data collection for analysis. The MD EXAFS spectra were averaged over the 1000 configurations with each configuration separated by 100 time steps.

III. Results and Discussion

The optimized ion−water potential parameters (i.e., Lennard Jones) were obtained by carrying out a series of MD simulations. During the simulation, the ion−water Lennard Jones parameters were modified until the calculated solvation enthalpies and hydration numbers reproduced the experimental measurements. The final potential parameters for the Ca^{2+} and Sr^{2+} ions and for the water model are listed in Table 1.

In Figure 1, we show the ion−water interaction energy for both ions and the minimum energy as a function of the separation distance. The minimum energies as well as the ion−water distances were in good agreement with the results obtained from ab initio molecular orbital theory calculations.[12] The calculated radial distribution functions, RDFs for the Sr^{2+}−H_2O and Ca^{2+}−H_2O systems are also included in Figure 1. The following observations are in order. The Sr−O and Ca−O RDFs are quite narrow with well-defined first and second hydration shells that are indicative of the strong interactions among these species. The coordination number obtained by integration of the first peak in the RDF out to its first minimum are 6.8 and 7.9 for Ca^{2+} and Sr^{2+}, respectively, which are in excellent agreement with results from recent experimental measurements of 7 and 8.[13,14] The hydration enthalpies, calculated using a method described previously,[15] are also in good agreement with the experimental values.[16] The simulated peak positions, coordination numbers, and hydration enthalpies are summarized in Table 2, along with the available experimental data. Having thus first established the good agreement between simulation results and both the experimental and ab initio data, we move on the to use the simulated hydration structure to compute the MD-EXAFS spectra for dilute Ca^{2+} and Sr^{2+} in solution.

The relation between the details of intermolecular potential and a prediction of EXAFS spectra builds on our previous work in MD-EXAFS, where an ensemble of molecular configurations are generated from the intermolecular potential and used in electron scattering analysis.[5,17] In the present work, we employ an updated version of the efficient algorithm for evaluating the

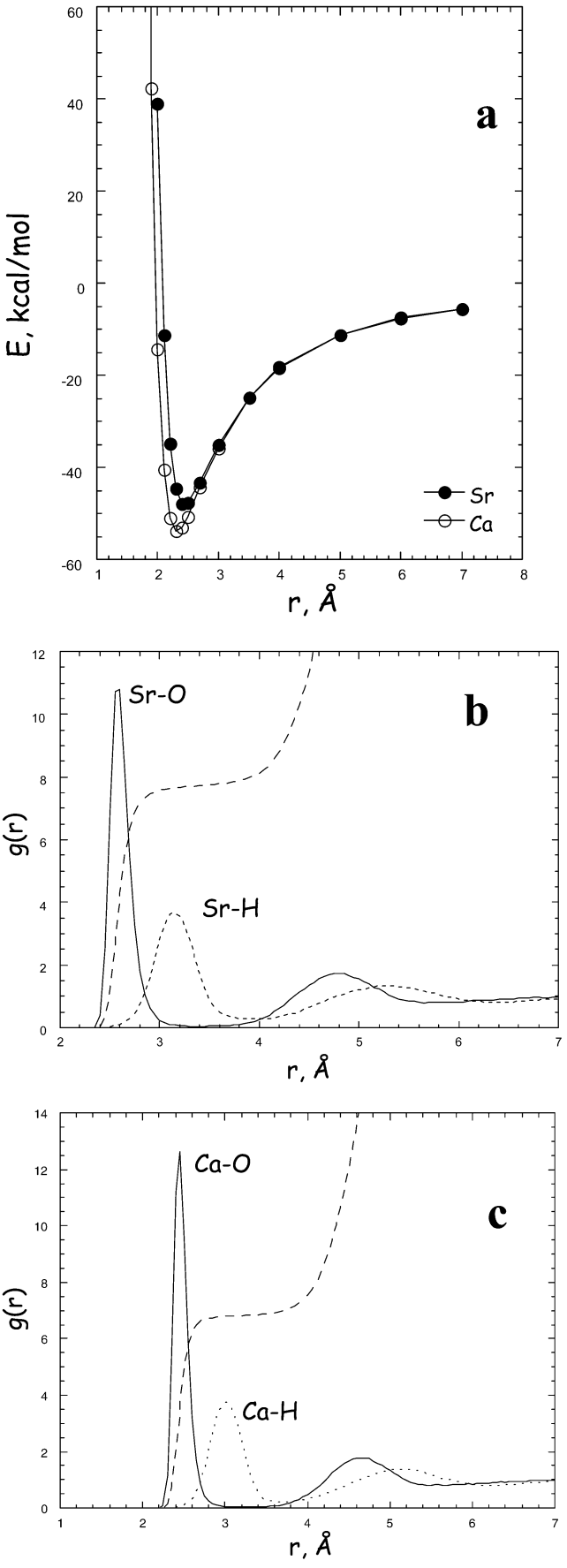

Figure 1. (a) Optimized ion−water interactions for Sr^{2+}−H_2O and Ca^{2+}−H_2O, (b) Simulated ion−water RDFs for Sr−O and Sr−H, and (c) Simulated ion−water RDFs for Ca−O and Ca−H.

TABLE 2: Structural and Thermodynamic Properties of (A) Sr^{2+} and (B) Ca^{2+} in Water at 300 K

	MD	expt
	A. Sr^{2+}	
R_{SrO} (Å)	2.60	2.63[a]
R_{SrH} (Å)	3.15	3.18[a]
coordination number	7.9	7.8[b],8.7[a]
ΔH_{sol} (kcal/mol)	-346 ± 3	-347[c]
	B. Ca^{2+}	
R_{CaO} (Å)	2.45	2.43[d]
R_{CaH} (Å)	3.00	2.94[d]
coordination number	6.8	6.8[d]
ΔH_{sol} (kcal/mol)	-370 ± 3	-378[e]

[a] Reference 14. [b] Reference 23. [c] Reference 16. [d] Reference 13. [f] Reference 16.

electron multiple scattering series by Rehr, Albers, and Zabinsky,[18] as it is implemented in the code FEFF8.[19] In standard EXAFS analysis, the fine structure factor is defined by

$$\chi(E) = \frac{\mu(E) - \mu_0(E)}{\Delta\mu_0(E_0)} \tag{1}$$

where $\mu(E)$ is the absorption coefficient as a function of X-ray energy E, $\mu_0(E)$ is the background absorption coefficient, and $\Delta\mu_0(E_0)$ is the jump in the absorption background at the absorption edge, E_0. Given a set of neighboring atoms located at positions $\mathbf{r}_i$ relative to the photoelectron source located at $\mathbf{r}_0$, with $R_i = |\mathbf{r}_i - \mathbf{r}_0|$

$$\chi(k) = \sum_i S_0{}^2 \frac{F_i(k)}{kR_i{}^2} e^{-2R_i/\lambda} \sin[2kR_i + \varphi_i(k)] \tag{2}$$

where the photoelectron wave-vector, k, is related to the X-ray energy by $E = E_0 + (\hbar^2k^2/2m_e)$. The effective backscattering amplitude, $F_i(k)$, and the phase shift, $\varphi_i(k)$, are determined from multiple scattering analysis. The mean free path, λ, accounts for inelastic scattering effects, whereas the many body amplitude reduction factor, $S_0{}^2$, accounts for many body effects in a single particle theory. The k^3-weighted $\chi(k)$ were Fourier transformed to obtain radial structure functions. For both the Ca and Sr systems, the K-edge excitation was probed.

In the calculations, a maximum path length of 4.5 Å was considered. The advanced features of the current version of FEFF 8.20 were employed, taking advantage of self-consistent potentials. FEFF's automated self-consistent potential calculation with a radius of 3.1 Å for the full multiple scattering during the self-consistency loop was employed. The average EXAFS spectrum was obtained from a configurational average

$$\bar{\chi}(k) = \frac{\bar{\mu}(E) - \mu_0(E)}{\Delta\mu_0(E_0)} \tag{3}$$

where bars denote a configurational average of eq 1. The configurational average is often fitted to the expression

$$\bar{\chi}(k) = \sum_i N_i S_0{}^2 \frac{\bar{F}_i(k)}{k\bar{R}_i{}^2} e^{-2\bar{R}_i/\lambda - 2k^2\sigma^2} \sin\left[2k\bar{R}_i + \bar{\varphi}_i(k) - \frac{4}{3}C_{3,i}k^3\right] \tag{4}$$

In this expression, $\bar{F}_i(k)$ is often estimated from a single characteristic configuration and assumed to have insignificant fluctuations with configuration. The Debye−Waller factor, $\sigma_i{}^2$, and the third cumulant, $C_{3,i}$, reflect the structural disorder of the system.

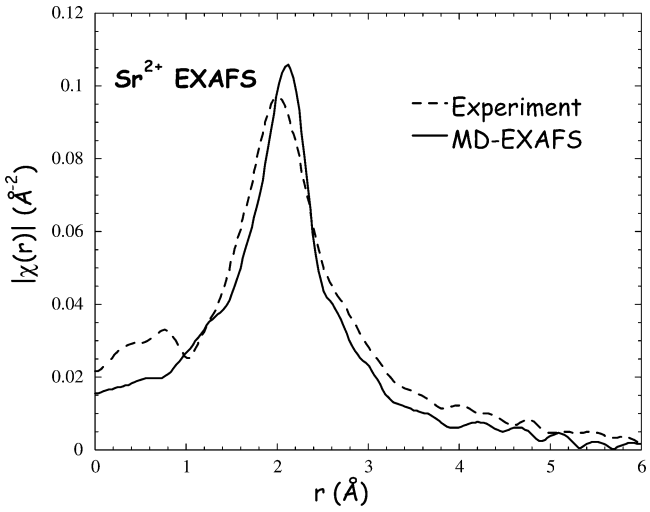

Figure 2. Comparison between the MD-EXAFS spectrum for Sr^{2+} in water and the corresponding experimental measurement.

To obtain a real space representation of the EXAFS spectra, we calculated the Fourier transform of the structure factor as implemented in the FEFFIT package[20]

$$\tilde{\chi}(R) = \frac{1}{\sqrt{2\pi}} \int_0^\infty k\chi(k)W(k)e^{i2kR}\, dk \tag{5}$$

where $W(k)$ is a Hanning window,[21]

Experimental and simulated spectra were transformed in an identical manner for direct comparison. $\tilde{\chi}(R)$ reduces to a series of peaks centered at the atomic distances, R_i, in the limit that $F_i(k)$ and $\varphi_i(k)$ do not depend on k. Aside from the distortion due to electron scattering and phase shift described in eq 2, $\tilde{\chi}(R)$ is a direct measurement of the radial probability, $4\pi R^2 g(R)$, in the region of the first solvation shell.

A cluster of the 10 closest water molecules to the photoelectron source was extracted from the configuration file from the MD simulation. This number ensured a good representation of the first solvation shell by reproducing the computed liquid ion−water RDF. When more molecules were included in the configuration averaged evaluation of the EXAFS signal, no significant effect was observed. This is due to the fact that configurational disorder in the second and higher solvation shells dampens their direct contribution to the EXAFS signal. Note that their indirect influence on the simulated structure of the first solvation shell is fully taken into account. In Figure 2, we display a comparison of $|\tilde{\chi}(R)|$ computed from the MD generated ensemble (MD-EXAFS) and the corresponding quantity derived from experimental measurement[14] for the case of Sr^{2+} in aqueous solution. $S_0{}^2$ was set to 0.85, to be consistent with the analysis of ref 13. In Figure 3, we display the same information for the case of Ca^{2+} in aqueous solution. In this case, $S_0{}^2$ was set to 0.69, again to be consistent with the analysis of ref 13. We first note that the overall agreement between experiments and calculations is quite satisfactory. In particularly, the MD-EXAFS spectrum for the dilute Sr^{2+} in aqueous solution is nearly quantitative agreement with the corresponding experimental measurement. This result is expected because we have demonstrated earlier in Table 2A, that the computed hydration properties of Sr^{2+} in aqueous solution give excellent agreement with the experimental results.

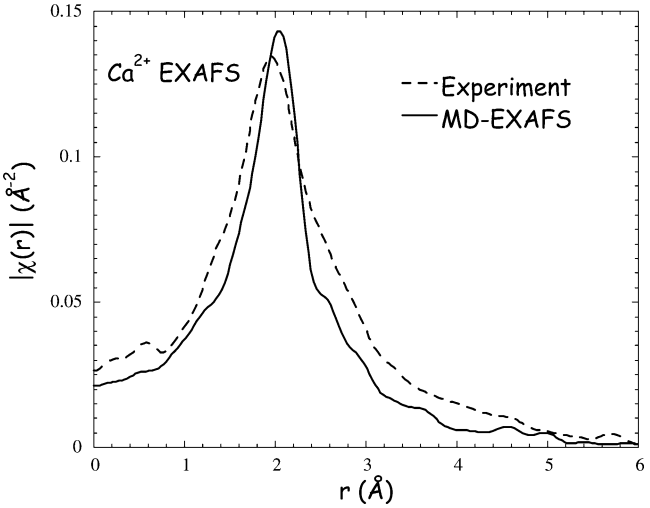

Figure 3. Same as Figure 2 for Ca^{2+}.

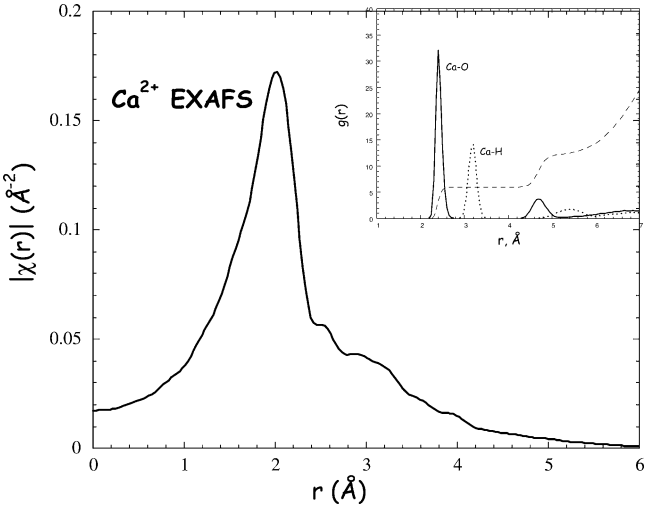

Figure 4. MD-EXAFS spectrum for Ca^{2+} in liquid methanol. The inset is the calculated Ca−O and Ca−H RDFs.

The key feature is the location of the peak of this distribution between 1 and 3 Å. The mean of this distribution agrees within 0.2 Å between the measurement and the simulation for both cases as expected from the agreement between the mean of the ion−water distances. The width of the peak is slightly larger for the measurement when compared to the simulation results. This indicates that width of the first peak of the ion-O $g(r)$ from the MD simulation is a smaller than the $g(r)$ that would be consistent with the EXAFS experiment for both cases. The extension of the current classical statistical mechanics analysis of the ion water structure to a quantum statistical treatment may improve agreement with the experimental measurement as quantum delocalization tends to broaden the radial distribution. The extent of this effect is a subject of further investigation. In addition, the sharpness of the peaks of the simulated ion−water RDF is associated with the repulsive r^{-12} term of the Lennard-Jones used to describe the short-range interactions between the ion−water. Our preliminary results indicated that, by replacing the repulsive r^{-12} term with a corresponding exponential term, the agreement of the computed Debye−Waller factor with the experimental result is improved about 10%. Research in this direction is underway. The Lennard-Jones potential parameters describing the ion−water interaction can be adjusted to obtain accurate enthalpy and distance information, but this functional form may not be capable of accurately describing the secondary details of the hydration structure.

In Table 2, we see that the simulation accurately reproduces both the ion−oxygen and the ion−hydrogen distances for water in the first shell about Sr^{2+} and Ca^{2+}. Notably, in both cases, the ion-hydrogen distance is considerably shorter than for a water molecule oriented in the "dipole" position where the water dipole moment is oriented perpendicular to the ion surface. In the "dipole" position, the ion−proton distances would be $R_{SrH} = 3.27$ Å and $R_{CaH} = 3.13$ Å. The wagging and rocking motions of the water on the ion surface lead to the shorter mean ion−hydrogen distances measured in both the simulation and the experimental XAFS. Significantly, the simulation accurately captures this structural detail without invoking a site-specific, oxygen "lone-pair" interaction with the cation.

Results of simulated MD-EXAFS of the dilute Sr^{2+} and Ca^{2+} in water mentioned above are quite reasonable, so we pursued the solvation structure of Ca^{2+} in another hydrogen-bonded solvent, methanol. Liquid methanol is of fundamental interest in the physical and chemical sciences and also of significant importance in technical and industrial applications. Methanol is the simplest alcohol and is a close analogue to water, because of the presence of a hydroxyl group. The major difference between water and methanol in the liquid state is that water molecules formed a tetrahedral coordinate, whereas the methanol molecules form clusters consisting of chains or small rings. We have employed the same approaches used in the study of ion−water system and have developed a set of polarizable Ca^{2+}−CH_3OH potential models ($\sigma = 2.9489$ Å, $\epsilon = 0.1$ kcal/mol, and $\alpha = 0.47$ Å^3) that reproduce the hydration properties of a dilute Ca^{2+} methanol solution. In this study, we used our recently developed polarizable potential model for CH_3OH−CH_3OH, which describes reasonably well the structure and thermodynamic properties of the bulk and the liquid/vapor interface of methanol.[22] In Figure 4, we show the calculated RDFs for the Ca^{2+}−CH_3OH system. We found the Ca−O ($R = 2.40$ Å) and Ca−H ($R = 2.34$ Å) RDFs are quite narrow with well-defined first and second hydration shells that are indicative of the strong interactions among these species. The coordination number obtained by integration of the first peak in the RDF, out to its first minimum is about 6. Also in Figure 4 we display an EXAFS spectrum $|\tilde{\chi}(R)|$ for the Ca^{2+} in liquid methanol, as predicted from the MD generated ensemble. Although this spectrum is similar to that of the corresponding spectrum of Ca^{2+} in water, we found that the shoulder between 3 and 4 Å is not entirely due to direct scattering for the carbon atom. From initial analysis, the presence of this shoulder is due to a combination of multiple scattering paths involving combinations of O, H, and C. To the best of our knowledge, an experimental EXAFS spectrum for the Ca^{2+} in liquid methanol is not available. However, judging from the quality of potential models and approaches, we believe that the simulated spectrum of the Ca^{2+} in liquid methanol will be in line with the corresponding experimental measurements when they are measured.

IV. Conclusions

Using classical MD techniques and polarizable potential models, we presented in this paper a detailed study of the solvation structure of dilute Ca^{2+}- and Sr^{2+}−water solution and also Ca^{2+}−methanol solution. Ca^{2+} and Sr^{2+} were chosen because of their important in many biological processes and environmental problems, respectively. We developed a set of polarizable ion−solvent interactions that accurately describes the hydration enthalpy, the coordination numbers, and the peak

locations of the ion−solvent RDFs. Subsequently, the MD EXAFS spectra were calculated, and these were in good agreement with corresponding experimental measurements.

To the best of our knowledge, our work is the first simulation study of EXAFS that employs polarizable potential models. This is a significant advance in the simulation approach because the interactions between the ions and the media can be described more accurately and the solvent molecules can respond to the electric fields created by their environments in a very realistic way. In particular, we have provided a detailed description of the structures of solvated ions at a molecular level. Obtaining this information through simulation is an initial step in developing first-principle predictions of transport mechanisms in complex molecular systems.

As stated in the Introduction, several simulation studies similar to ours on ionic systems employing pair potential models have been carried out to calculate the MD EXAFS spectra. We can conclude that the inclusion of many-body polarization effects into the potential model does not interfere with the ability to predict the EXAFS spectra. It is not clear that pair potentials are sufficient to model ion solvation in clusters and at interfaces, whereas many-body polarization effects have been shown to be important in describing clusters and liquid interfaces.

Acknowledgment. This work was performed in the Environmental Molecular Sciences Laboratory (EMSL) at Pacific Northwest National Laboratory under the auspices of the Division of Chemical Sciences, Office of Basic Energy Sciences, U.S. Department of Energy. Pacific Northwest National Laboratory is operated by Battelle for the Department of Energy. Computer resources were provided by the Division of Chemical Sciences and by the Scientific Computing Staff, Office of Energy Research, at the National Energy Research Supercomputer Center (Berkeley, California). Operation of EMSL is supported by DOEs Office of Biological and Environmental Research.

References and Notes

(1) Allen, M. P.; Tildesley, D. J. C*omputer Simulations of Liquids*; Clarendon Press: Oxford, U.K., 1987.

(2) Chazin, W. J. *Struct. Biol.* **1995**, *2*, 707.

(3) Haag, W. R.; Yao, C. C. D. *Environ. Sci. Technol.* **1992**, *26*, 1005; US Department of Energy, Office of Environmental Management, FY 1995 Technology Development Needs Summary, 1994; p. 2−17.

(4) Dang, L. X.; Chang, T−M. *J. Phys. Chem. B* **2002**, *106*, 235.

(5) Palmer, B. J.; Pfund, D. M.; Fulton, J. L. *J. Phys. Chem.* **1996**, *100*, 13393.

(6) Jalilehvand, F.; Spangbeg, D.; Lingqvist-Reis, P.; Hermansson, K. P.; Persson, I.; Sandstrom, M. *J. Am. Chem. Soc.* **2001**, *123*, 431.

(7) Roccatano, D.; Berendsen, H. J. C.; D'Angelo, P. *J. Chem. Phys.* **1998**, *108*, 9487.

(8) Dang, L. X.; Chang, T−M. *J. Chem. Phys.* **1997**, *106*, 8149.

(9) Berendsen, H. J. C.; Postma, J. P.; Di Nola, A.; Van Gunsteren, W. F.; Haak, J. R. *J. Chem. Phys.* **1984**, *81*, 3684.

(10) Rykaert, J. P.; Ciccotti, G.; Berendsen, H. J. C. *J. Comput. Phys.* **1977**, *23*, 327.

(11) Perara, L.; Essmann, U.; Berkowitz, M. *J. Chem. Phys.* **1995**, *102*, 450. Spohr, E. *J. Chem. Phys.* **1997**, *107*, 6342.

(12) Glendening E. D.; Feller D. *J. Phys Chem.* 1**996**, *100*, 4790.

(13) Fulton, J. L.; Heald, S. M.; Badyal, Y. S.; Simonson, J. M. *J. Phys. Chem. A* **2003**, *107*, 4688.

(14) Data for Sr^{2+} was acquired and analyzed using exactly the same methods described in ref 13 for the Ca^{2+} with an estimated $S_0^2 = 0.85$.

(15) Dang, L. X.; Rice, J.; Caldwell, J.; Kollman, P. A. *J. Am. Chem. Soc.* **1991**, *113*, 2481.

(16) Marcus, Y. *Ion Solvation*; John Wiley & Sons Limited: London, 1985.

(17) McCarthy, M. I.; Schenter, G. K.; Chacon Taylor, M. R.; Rehr, J. J.; Brown, G. E. *Phys. Rev. B* **1997**, *56*, 9925. Campbell, L.; Rehr, J. J.; Schenter, G. K.; McCarthy, M. I.; Dixon, D. *J. Sync. Rad.* **1999**, *6*, 310.

(18) Rehr, J. J.; Albers, R. C.; Zabinsky, S. I. *Phys. Rev. Lett.* **1992**, *69*, 3397.

(19) Ankudinov, A. L.; Bouldin, C.; Rehr, J. J.; Sims, J.; Hung, H. *Phys. Rev. B* **2002**, *65*, 104107.

(20) Newville, M.; Ravel, B.; Haskel, D.; Rehr, J. J.; Stern, E. A.; Yacoby, Y. *Physica B* **1995**, *208&209*, 154.

(21) $W(k) = \sin^2(\pi(k - k_{min} + \Delta k/2)/2\Delta k)$ for $k_{min} - \Delta k/2 \leq k < k_{min} + \Delta k/2$, $W(k) = 1$ for $k_{min} + \Delta k/2 \leq k \leq k_{max} - \Delta k/2$, and $W(k) = \cos^2(\pi(k - k_{max} + \Delta k/2)/2\Delta k)$ for $k_{max} - \Delta k/2 < k \leq k_{max} + \Delta k/2$. We set $k_{min} = 4$ Å^{-1}, $\Delta k = 1$ Å^{-1}, and $k_{max} = 13$ Å^{-1}.

(22) Dang, L. X.; Chang, T−M. *J. Chem. Phys.* **2003**, *119*, 9857.

(23) Seward, T. M.; Henderson, C. M. B.; Charnok, J. M.; Driesner, T. *Geochim. Cosmochim. Acta* **1999**, *63*, 2409.